Detection of Lipid in Abdominal Tissues with Opposed-Phase Gradient-Echo Images at 1.5 T: Techniques and Diagnostic Importance[1]

Eric K. Outwater, MD
Roberto Blasbalg, MD
Evan S. Siegelman, MD
Marc Vala, MD

T1-weighted gradient-echo magnetic resonance images can be acquired with an echo time such that water and lipid spins are in phase or opposed phase. Observation of relative loss of signal intensity on opposed-phase images compared with that on in-phase images allows qualitative assessment of relatively small amounts of lipid in tissues. Conversely, frequency-selective fat saturation techniques are useful primarily for identifying predominantly fatty masses such as angiomyolipomas. Both in-phase and opposed-phase images should be acquired with similar parameters because unequivocal identification of lipid requires comparison with in-phase images to control for T1 and T2* effects. Opposed-phase imaging has been used to differentiate adrenal adenomas, which contain lipid, from adrenal metastases, which do not. The technique can be expanded to examine a spectrum of intraabdominal tumors and conditions that are characterized by intracellular lipid. These include hepatic steatosis, hepatocellular neoplasms, myelolipoma, adrenocortical carcinoma, angiomyolipoma, and renal cell carcinoma. In liver masses, the presence of lipid is largely restricted to primary hepatocellular tumors. Renal and adrenal masses may contain focal fat (angiomyolipomas and myelolipomas, respectively) or diffuse lipid (clear cell renal carcinomas and adenomas, respectively).

Abbreviation: TE = echo time

Index terms: Adrenal gland, neoplasms, 86.30 • Fat, MR • Kidney neoplasms, MR, 81.30, 81.121412, 81.121415 • Liver, fatty, 761.50 • Liver neoplasms, MR, 761.30, 761.121412, 761.121415 • Magnetic resonance (MR), fat suppression, ••.121415[2]

RadioGraphics 1998; 18:1465–1480

[1]From the Departments of Radiology (E.K.O., R.B.) and Pathology (M.V.), Thomas Jefferson University Hospital, 132 S 10th St, Ste 1096, Philadelphia, PA 19107-5244; and the Department of Radiology, University of Pennsylvania Medical Center, Philadelphia (E.S.S.). Presented as a scientific exhibit at the 1997 RSNA scientific assembly. Received December 3, 1997; revision requested February 3, 1998, and received February 24; accepted March 17. **Address reprint requests to** E.K.O.

[2]•• indicates multiple body systems.

■ INTRODUCTION

Methods for selective magnetic resonance (MR) imaging of fat or water were first developed for spin-echo sequences by altering the interval of the refocusing pulse relative to the readout gradient; this technique became known as the Dixon method of spectroscopic imaging (1). Quantitative or qualitative estimates of fat in tissues could be obtained by comparing the in-phase image (a standard spin-echo T1-weighted image) with the opposed-phase image (a spin-echo T1-weighted image with fat and water signals at 180° [opposite phase] at the echo time [TE]). This technique was employed to quantitate fat in tissues (2,3) or improve fat suppression by using frequency-selective pulses (4,5). However, the spin-echo technique of obtaining in-phase and opposed-phase images is time-consuming, is susceptible to respiratory and other motion artifacts, and requires software modifications.

Gradient-echo images can replace spin-echo images for T1-weighted imaging in the upper abdomen. Gradient-echo sequences are performed with suspended respiration to reduce motion artifacts and are faster to shorten the overall examination time and improve temporal resolution in dynamic gadolinium-enhanced studies. Unlike spin-echo images, gradient-echo images are intrinsically in-phase, opposed-phase, or somewhere in between depending on the TE. Understanding the opposed-phase effect on these routine T1-weighted images can prevent errors based on artifacts of these images. Furthermore, controlling the chemical shift effect, specifically to obtain in-phase and opposed-phase images for comparison, provides additional diagnostic information in a variety of abdominal disorders.

In this article, the technique of opposed-phase gradient-echo and fat saturation imaging is described. Some pitfalls in the interpretation of opposed-phase images and examples of the diagnostic importance of identifying lipid in tissues and masses in the abdomen are also presented.

■ OPPOSED-PHASE GRADIENT-ECHO AND FAT SATURATION IMAGING

Opposed-phase gradient-echo images differ from in-phase images in two respects: a slight difference in TE and a 180° phase difference between lipid and water spins because of the difference in the chemical shifts of lipid and water. In spin-echo images and in-phase gradient-echo images, the signals from water and triglyceride are in phase relative to each other and so these signals contribute additively to the net signal intensity obtained from each voxel. The phases of water and triglyceride are opposite on gradient-echo images obtained with an appropriate TE (6). Because there is no 180° refocusing pulse to rephase different resonant frequencies within a voxel, the phases of water and triglyceride cycle in and out of phase as TE changes. At 1.5 T, TEs of approximately 2.1, 6.3, and 10.5 msec yield opposed-phase images and TEs of 4.2, 8.4, and 12.6 msec yield in-phase images. Relative to the signal intensity on similar in-phase images, the loss of signal intensity on opposed-phase images is maximal when signal intensity due to lipid and water exists in equal proportions within a voxel and is minimal when the voxel tissue is predominantly fat or water (Fig 1).

To qualitatively detect lipid content in tissues with opposed-phase images, the in-phase images used for comparison should have identical parameters except for the TE. If the opposed-phase images have a longer TE than the in-phase images (eg, 6.3 msec for the opposed-phase images and 4.2 msec for the in-phase images), then interpretation of relative loss of signal intensity on the opposed-phase images is confounded by T2* decay within the tissue (7). Therefore, it is preferable to use a shorter TE to obtain the opposed-phase images. For quantitative measurements, in-phase and opposed-phase images can be used to calculate the fraction of fat in tissues by using an appropriate repetition time and flip angle (8).

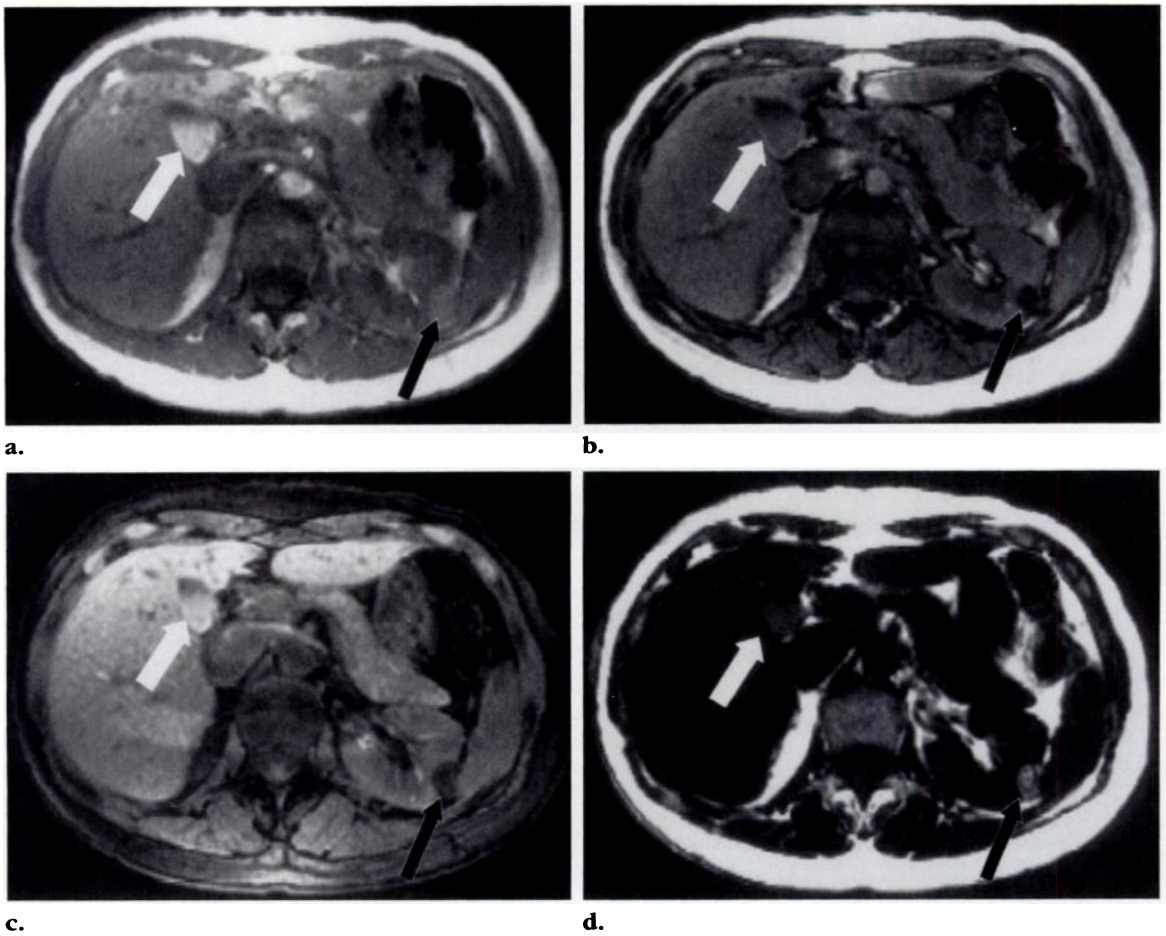

Figure 1. Renal angiomyolipoma in a 44-year-old woman. **(a)** In-phase T1-weighted MR image (repetition time msec/TE msec = 120/4.2) shows a hyperintense mass in the left kidney (black arrow). This degree of hyperintensity in a mass is consistent with fat or hemorrhage. Note the high signal intensity of the bile (white arrow). **(b)** Opposed-phase T1-weighted MR image (120/2.6) shows loss of signal intensity in the mass (black arrow), a finding that indicates a lipid composition. The bile (white arrow) also demonstrates signal intensity loss because of a lipid composition. **(c)** Fat saturation opposed-phase T1-weighted MR image (120/2.6) shows that the mass (black arrow) has markedly decreased signal intensity compared with that on the in-phase image **(a)**, a finding that indicates predominantly fatty tissue. In contrast, the bile (white arrow) does not demonstrate an appreciable change in signal intensity compared with that on the in-phase image **(a)** because the lipid content is less than that of the angiomyolipoma. **(d)** Water saturation T1-weighted MR image (120/4.2) shows remaining high signal intensity in the mass (black arrow), a finding that indicates fat. The bile (white arrow) also retains signal intensity because of a lipid composition.

Frequency-selective fat suppression techniques reduce the signal intensity from lipid-containing voxels and thus can be used for the detection of lipid (Fig 1). Similarly, frequency-selective water suppression imaging can yield similar information by reducing the signal intensity of water in tissues and showing residual signal intensity in fatty masses (Fig 1). Saturation techniques are appropriate when evaluating fatty masses such as dermoid cysts and angiomyolipomas (Fig 2). However, intracellular lipid is commonly present and responsible for a minority of the signal intensity in many tumors and

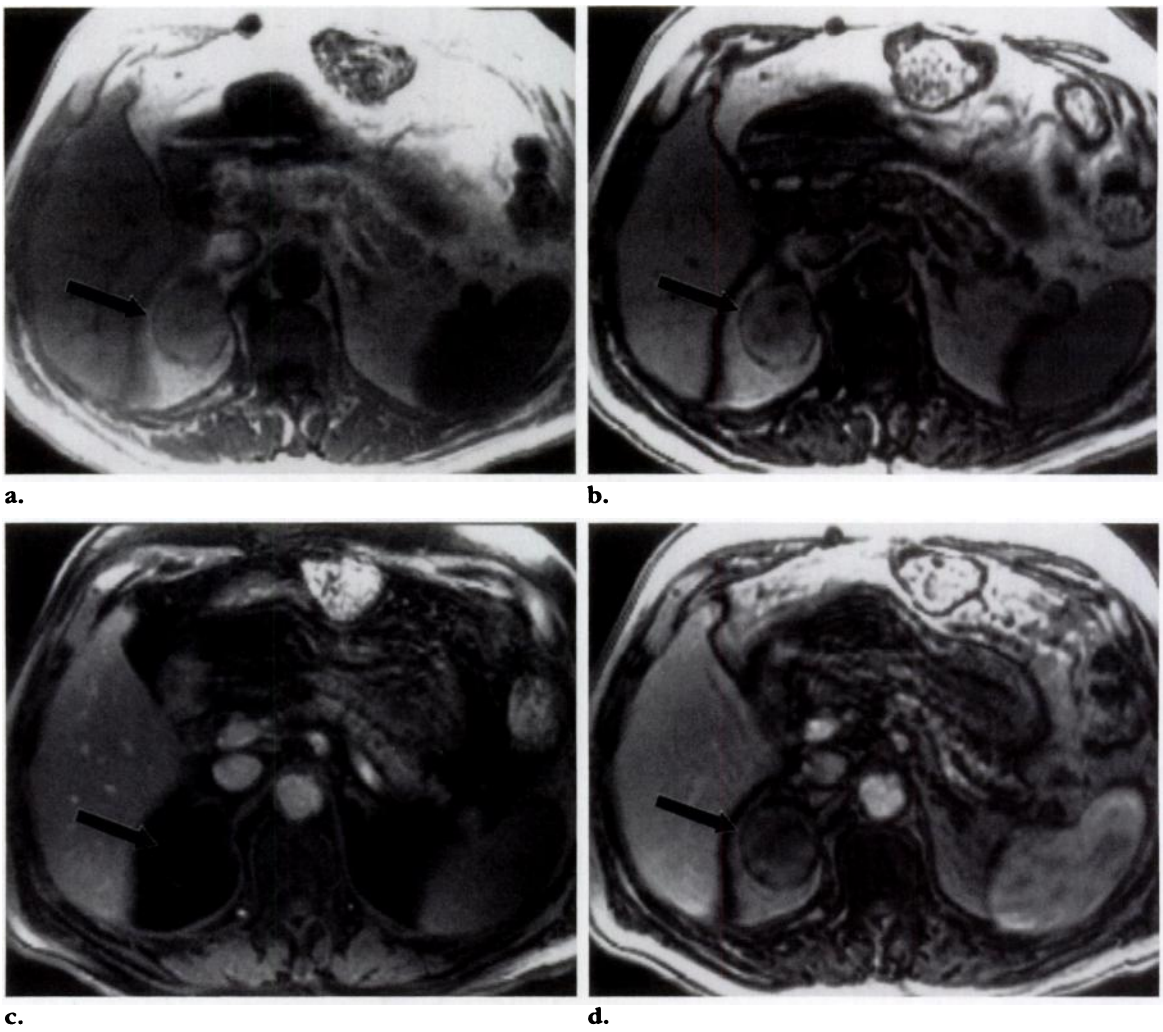

Figure 2. Myelolipoma of the adrenal gland in a 76-year-old man. **(a)** In-phase T1-weighted fast multiplanar spoiled gradient-echo MR image (120/4.2) shows a hyperintense right adrenal mass (arrow). **(b)** Opposed-phase T1-weighted fast multiplanar spoiled gradient-echo MR image (150/2.2) shows slight focal loss of signal intensity in the mass (arrow). **(c)** Fat saturation opposed-phase T1-weighted fast multiplanar spoiled gradient-echo MR image (140/2.2) shows signal intensity loss in the myelolipoma (arrow). **(d)** Gadolinium-enhanced opposed-phase T1-weighted fast multiplanar spoiled gradient-echo MR image (150/2.2) shows greater loss of signal intensity in the enhancing myelolipoma (arrow) than does the unenhanced opposed-phase image **(b)**.

tissues, and this lipid will be more sensitively detected with opposed-phase techniques. For example, consider a region of the liver where lipid accounts for 20% and water accounts for 80% of the signal intensity on an in-phase T1-weighted image. On a fat-suppressed image, 80% of the original signal intensity will remain. On a comparable opposed-phase image, the liver will show only 60% of the original signal intensity due to phase cancellation of the signal intensities of lipid and water. Therefore, opposed-phase images show more signal intensity loss in tissues containing relatively small quantities of lipid than do fat-suppressed images. Conversely, fat saturation images show greater signal intensity loss than do opposed-phase images in predomi-

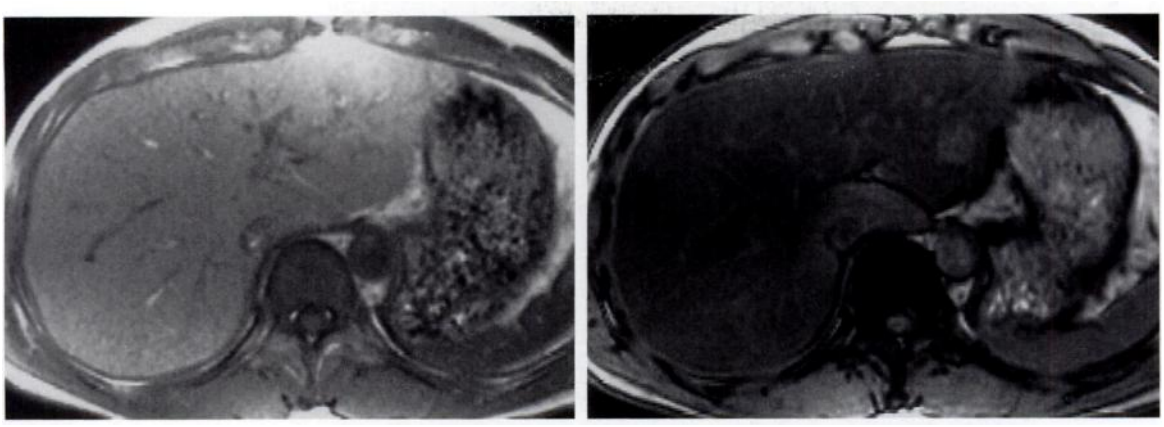

a. b.

Figure 3. Diffuse fatty liver in a 48-year-old man. **(a)** In-phase T1-weighted fast multiplanar spoiled gradient-echo MR image (125/4.2) shows normal liver-spleen contrast with the liver hyperintense relative to the spleen. **(b)** Opposed-phase T1-weighted fast multiplanar spoiled gradient-echo MR image (160/2.3) shows that the liver is moderately hypointense relative to the spleen, a finding that indicates diffuse hepatic steatosis. There is comparatively less fatty infiltration of the caudate lobe.

nantly fatty tissue (Fig 2). However, the "etching" or "India ink" artifact, which occurs at fat-soft tissue interfaces on opposed-phase images, will still allow identification of fatty tissue on opposed-phase images even if the signal intensity loss is subtle.

Understanding the opposed-phase effect can prevent misdiagnosis with MR images. For example, the use of opposed-phase images in dynamic gadolinium-enhanced imaging may lead to "paradoxical" signal intensity loss in enhancing tumors (9). If a tumor is predominantly fatty, such as an angiomyolipoma or myelolipoma, then shortening the T1 of the water component with gadolinium leads to greater longitudinal magnetization of the water component and thus greater opposed-phase cancellation of net signal intensity. Therefore, an enhancing myelolipoma will demonstrate loss of signal intensity compared with that on unenhanced images (Fig 2).

■ ABDOMINAL TUMORS AND CONDITIONS CHARACTERIZED BY INTRACELLULAR LIPID

• Hepatic Steatosis

Hepatic steatosis is associated with a wide variety of hepatic diseases and clinical situations, most commonly alcoholic steatohepatitis and obesity. Hepatic steatosis can be detected with ultrasound, computed tomography (CT), or conventional MR imaging. However, conventional spin-echo MR images are relatively insensitive in the detection of mild or moderate fatty infiltration. Opposed-phase images demonstrate relatively small amounts of fat deposition as loss of signal intensity relative to that on in-phase images (3,10,11) (Fig 3). Acquisition of

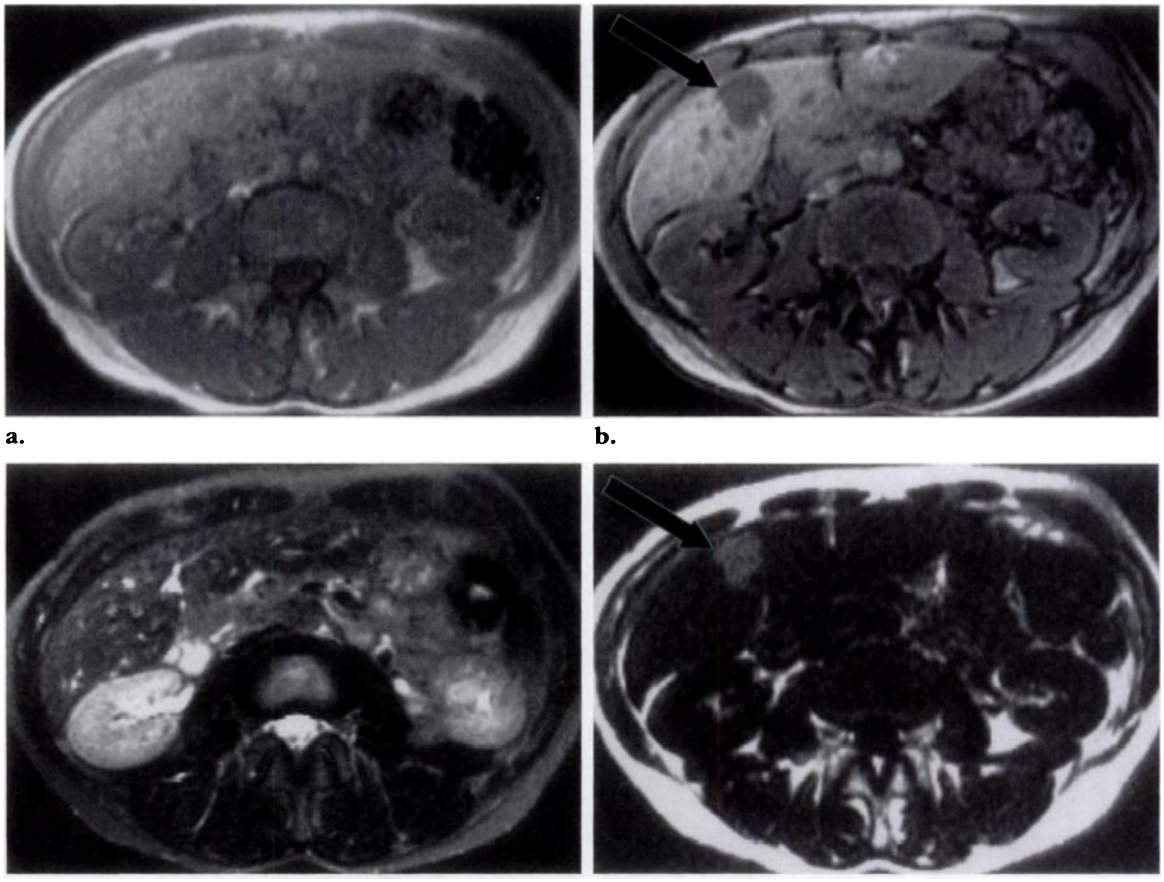

Figure 4. Focal fatty infiltration of the liver in a 50-year-old woman. **(a)** In-phase T1-weighted fast multiplanar spoiled gradient-echo MR image (150/4.2) shows normal signal intensity of the liver. **(b)** Opposed-phase T1-weighted fast multiplanar spoiled gradient-echo MR image (150/2.1) shows an area that is hypointense relative to the adjacent liver tissue (arrow), a finding that indicates steatosis. **(c)** T2-weighted fast spin-echo MR image (6,000/99) shows no abnormality that would indicate an underlying mass. **(d)** Water saturation T1-weighted MR image (150/4.2) shows an area in the right lobe that is slightly hyperintense relative to the adjacent liver tissue (arrow), a finding that also indicates focal fatty infiltration.

both opposed-phase and in-phase images prevents focal sparing or steatosis from obscuring lesions or mimicking a lesion (12) (Fig 4). Inhomogeneous fatty infiltration may be caused by differential portal venous flow (and delivery of fatty acids or alcohol) to segments of the liver. Partial obstruction of the portal vein will cause diminished fatty infiltration in the affected segment (Fig 5).

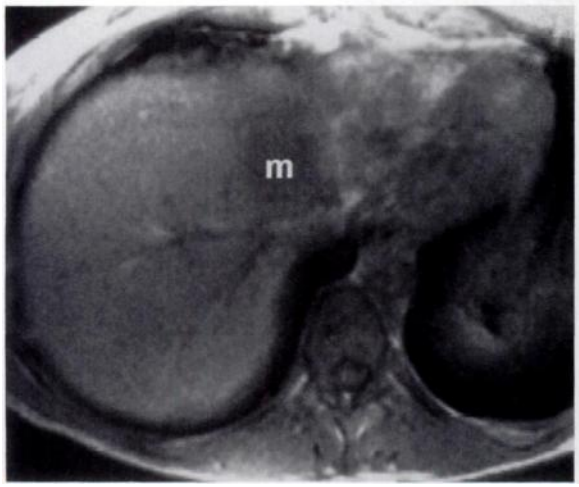

a.

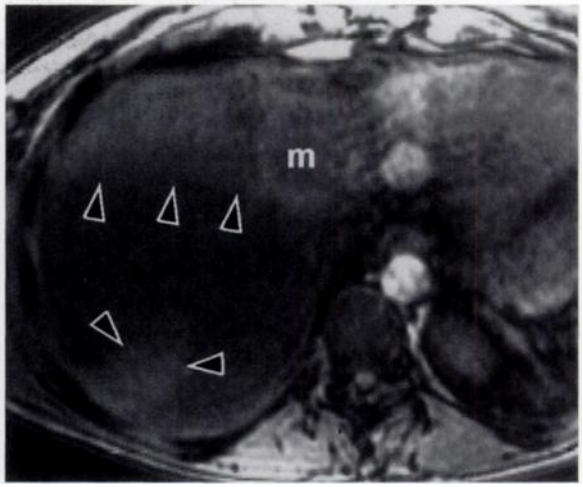

b.

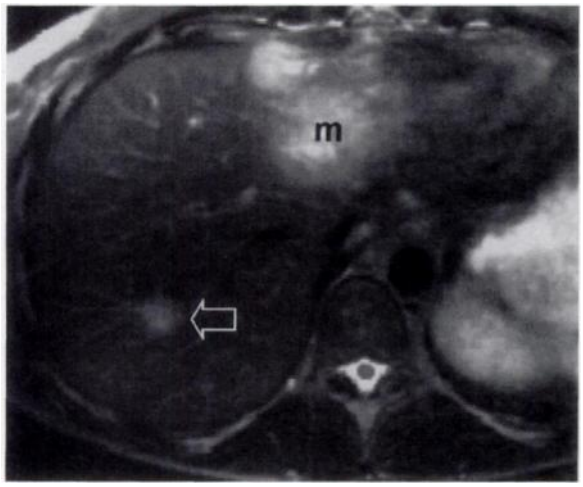

c.

Figure 5. Focal fatty infiltration of the liver because of obstructed portal venous flow from metastases in a 46-year-old woman. **(a)** In-phase T1-weighted fast multiplanar spoiled gradient-echo MR image (120/4.2) shows normal signal intensity in the right hepatic lobe. Metastases (*m*) are seen in the left lobe. **(b)** Opposed-phase T1-weighted fast multiplanar spoiled gradient-echo MR image (150/2.2) shows decreased signal intensity in the right lobe, a finding that indicates steatosis. Wedge-shaped areas of relatively spared parenchyma are seen in the left lobe and part of segment 7 (arrowheads). *m* = metastases. **(c)** T2-weighted fast spin-echo MR image (10,000/96 [effective]) obtained slightly inferior to **a** and **b** shows an obstructing metastasis of the right lobe (arrow). The wedge-shaped area in the right lobe does not represent a tumor but results from proximal partial obstruction of the portal vein and increased arterial flow. *m* = metastases.

One disadvantage of use of gradient-echo sequences, in contrast to spin-echo sequences, for detection of lipid is that the results may be confounded by magnetic susceptibility effects. T2* signal dephasing will be more pronounced on longer TE images, specifically on the in-phase images (TE = 4.2) relative to the shorter TE opposed-phase images. Particularly in patients with iron deposition in the liver, the comparison of signal intensity between these two types of images will not be valid (Fig 6).

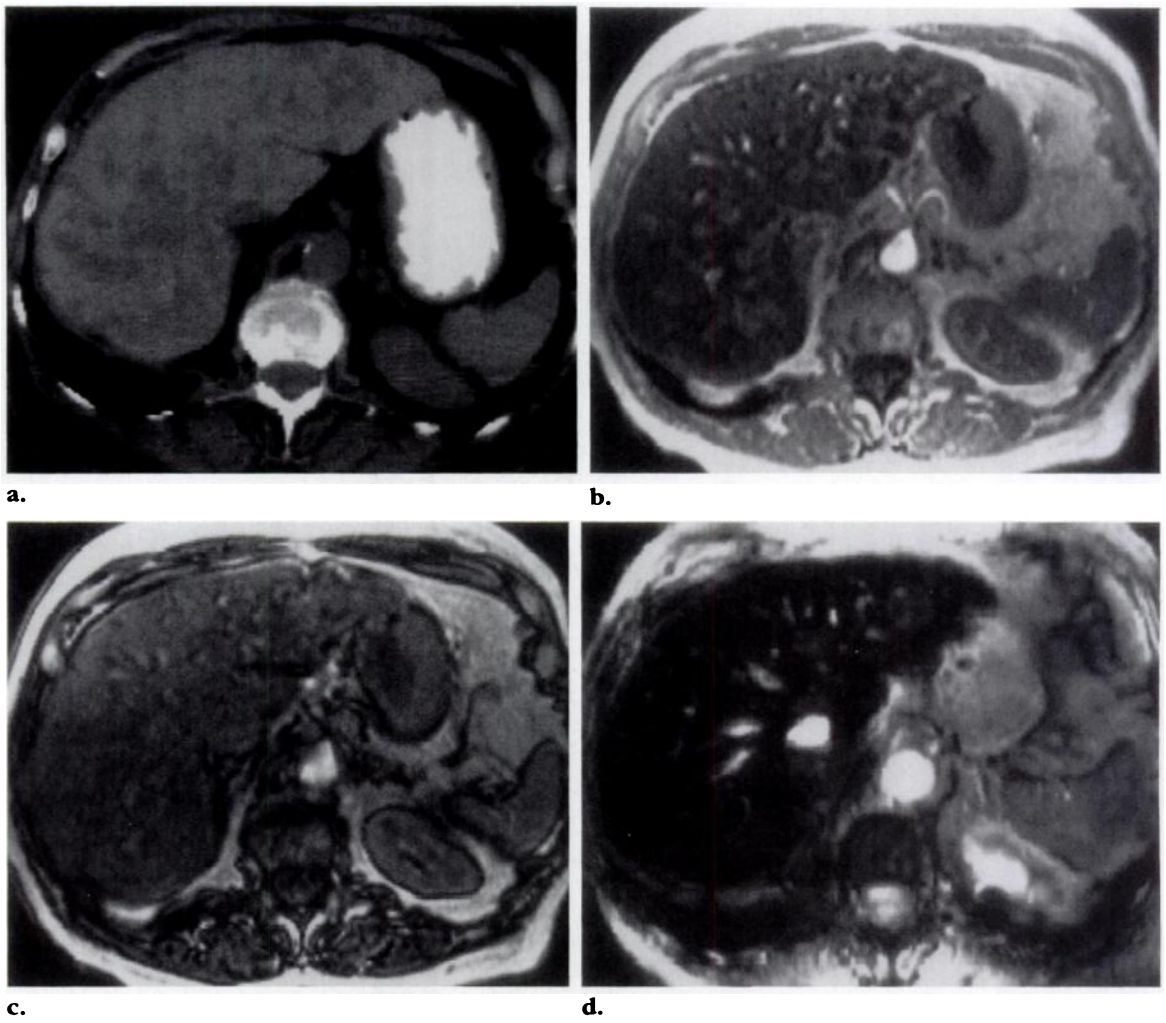

Figure 6. Biopsy-proved hepatic steatosis obscured at MR imaging by hemochromatosis in a 67-year-old woman. **(a)** CT scan obtained without intravenously administered contrast material shows hypoattenuating lesions throughout the liver. **(b)** In-phase T1-weighted fast multiplanar spoiled gradient-echo MR image (120/4.2) shows abnormally low signal intensity throughout the liver, but the discrete lesions seen on the CT scan **(a)** are not apparent. **(c)** Opposed-phase T1-weighted fast multiplanar spoiled gradient-echo MR image (120/2.6) shows increased signal intensity compared with that on the in-phase image **(b)** throughout the liver, a finding consistent with T2* effects. The steatosis is obscured by the T2* signal decay from the iron deposition within the liver. **(d)** Longer TE gradient-echo MR image (100/20) shows markedly low signal intensity in the liver from hemochromatosis.

• Liver Tumors

Variable degrees of intracellular lipid are occasional features of a number of hepatocellular tumors. Hepatic adenoma, hepatocellular carcinoma, and uncommonly focal nodular hyperplasia may demonstrate steatosis (13,14). On T1-weighted images, these tumors are often hyperintense relative to the surrounding liver tissue, although the high signal intensity is often not due to fatty infiltration.

Identification of lipid within a mass with opposed-phase imaging can narrow the differential diagnosis to hepatocellular tumors (12). Other hepatic tumors, such as metastases, cholangiocarcinoma, lymphoma, and hemangioma, do not demonstrate lipid on opposed-phase images. Fifty percent to 68% of hepatic adenomas demonstrate fatty change at MR imaging (15,16) (Fig 7). Fatty infiltration occurs in 14% of all hepatocellular carcinomas and in 30%–40% of those that are hyperintense on in-phase T1-weighted images (12,17) (Fig 8).

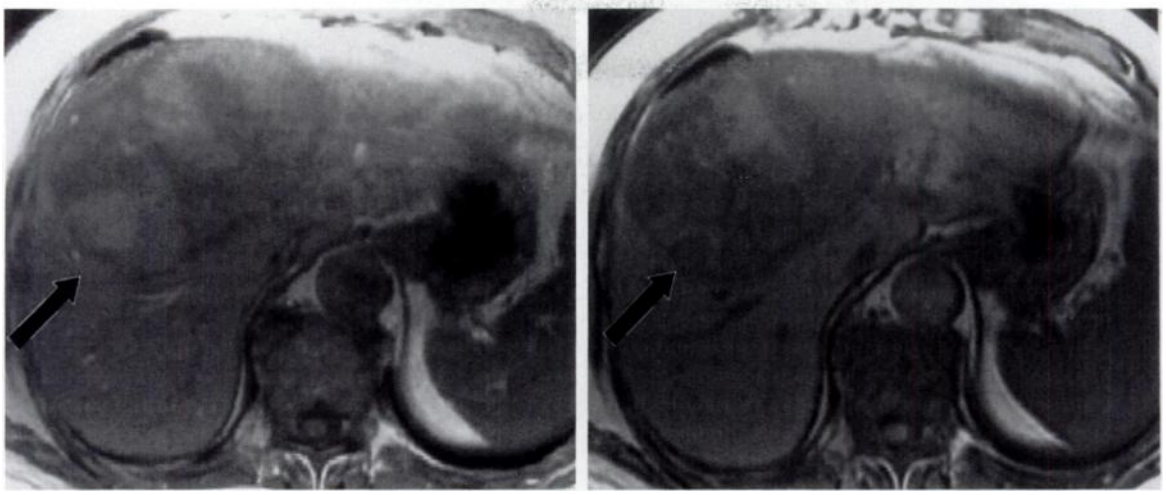

a. b.

Figure 8. Hepatocellular carcinoma in a 71-year-old man. **(a)** In-phase T1-weighted fast multiplanar spoiled gradient-echo MR image (120/4.2) shows a large, heterogeneous liver mass with an area that is slightly hyperintense (arrow) relative to the adjacent liver or tumor tissue. **(b)** Opposed-phase T1-weighted fast multiplanar spoiled gradient-echo MR image (150/1.8) shows that the hyperintense area on the in-phase image **(a)** has become hypointense (arrow) relative to the adjacent liver tissue, a finding that indicates steatosis within the tumor.

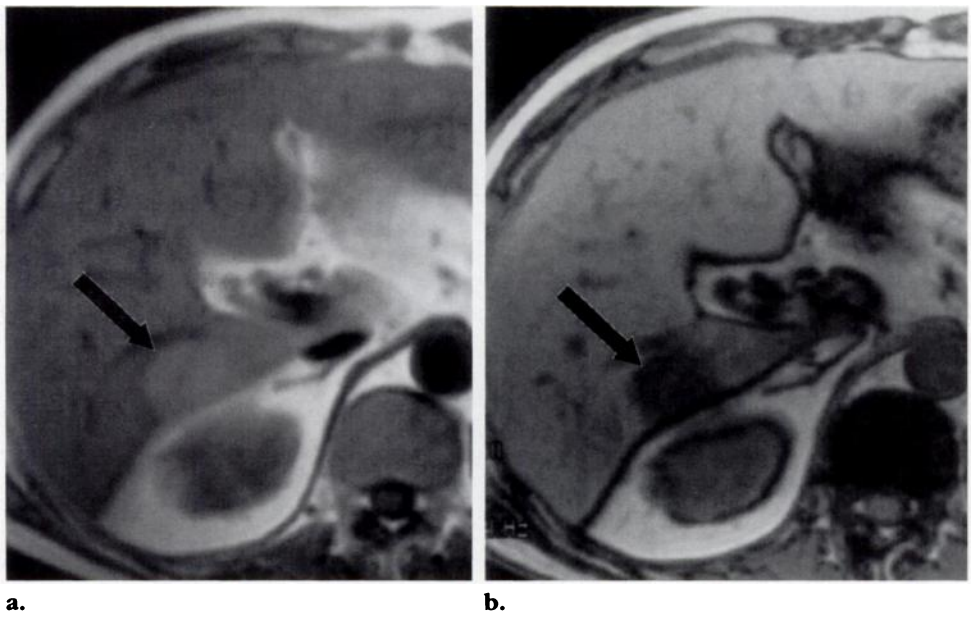

a. b.

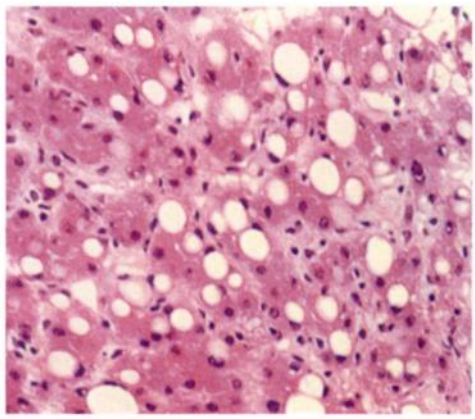

c.

Figure 7. Biopsy-proved hepatic adenoma in a 49-year-old man. **(a)** In-phase T1-weighted fast multiplanar spoiled gradient-echo MR image (120/4.2) shows a hyperintense liver mass (arrow). **(b)** Opposed-phase T1-weighted fast multiplanar spoiled gradient-echo MR image (150/1.5) shows decreased signal intensity of the mass (arrow), a finding that indicates steatosis within the tumor. **(c)** Photomicrograph (original magnification, ×100; hematoxylin-eosin stain) of a biopsy specimen from the tumor shows hepatic cells with scattered lipid droplets.

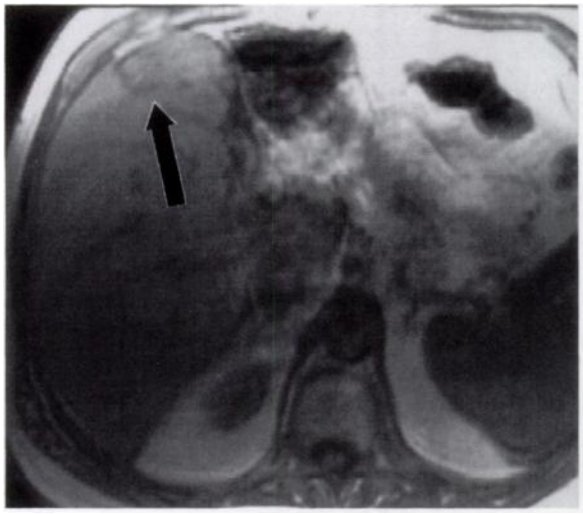

a.

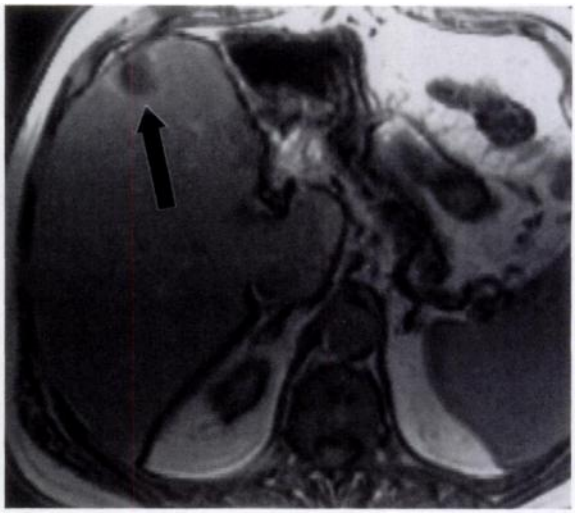

b.

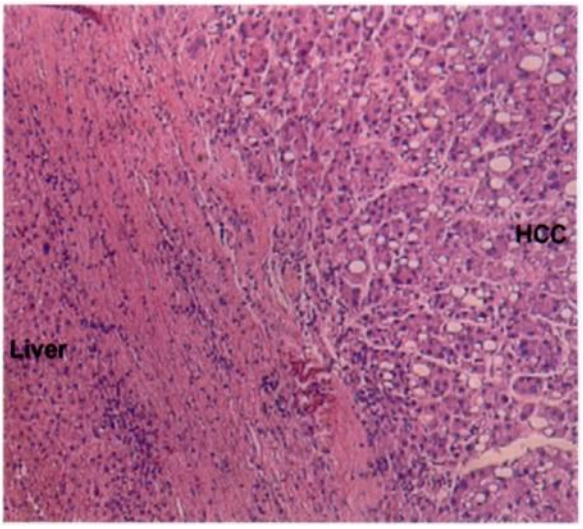

c.

Figure 9. Small hepatocellular carcinoma in a 76-year-old man. **(a)** In-phase T1-weighted fast multiplanar spoiled gradient-echo MR image (130/4.2) shows a small nodule (arrow) that is almost isointense relative to the surrounding liver tissue. **(b)** Opposed-phase T1-weighted fast multiplanar spoiled gradient-echo MR image (150/1.8) shows loss of signal intensity in the nodule, a finding that indicates steatosis within the tumor. **(c)** Photomicrograph (original magnification, ×40; hematoxylin-eosin stain) of the edge of the tumor shows numerous clear lipid droplets within the tumor (*HCC*). Steatosis is not seen in the adjacent liver tissue (*Liver*).

Early, well-differentiated hepatocellular carcinomas are often small and nondescript on T2-weighted images. Therefore, small tumors that demonstrate steatosis may be confused with focal fatty infiltration (Fig 9).

Hepatic angiomyolipomas and lipomas are uncommon and demonstrate focal fat, which can be detected with fat saturation images or opposed-phase images (18).

• Adrenal Masses

Comparison of in-phase and opposed-phase images allows identification of intracellular lipid in the majority of adrenal adenomas and adrenocortical nodules (19–24). Adrenal adenomas accumulate lipids used in the synthesis of steroid hormones. Signal intensity loss on opposed-phase images is a reliable sign of a benign adrenal mass such as an adenoma (Fig 10). With opposed-phase images, a sensitivity of approximately 80% for the diagnosis of adenoma by means of quantitative or qualitative criteria can be achieved with a specificity of close to 100% (19,21,23). Characterization of an adrenal mass

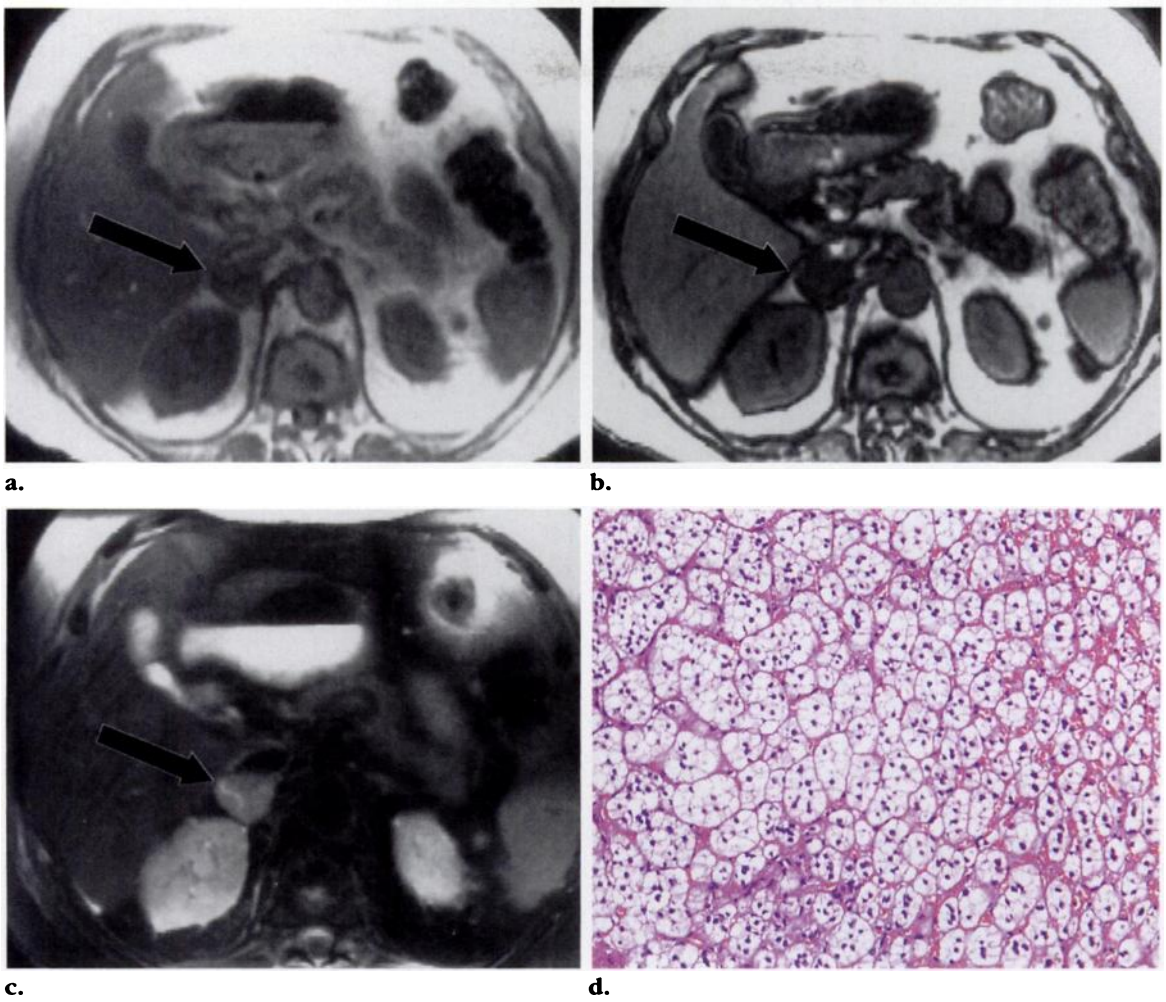

Figure 10. Adrenal adenoma and Cushing syndrome in a 59-year-old woman. **(a)** In-phase T1-weighted fast multiplanar spoiled gradient-echo MR image (100/4.2) shows a right adrenal mass (arrow) that is slightly hyperintense relative to the kidney. **(b)** Opposed-phase T1-weighted fast multiplanar spoiled gradient-echo MR image (100/2.3) shows that the mass (arrow) is hypointense relative to the liver or kidney, a finding that indicates lipid. **(c)** T2-weighted MR image (3,800/96) shows that the mass (arrow) is hyperintense relative to the liver. **(d)** Photomicrograph (original magnification, ×100; hematoxylin-eosin stain) of the mass shows adrenocortical cells with extensive clear cytoplasms, a finding consistent with lipid.

as benign obviates further follow-up studies or biopsy. The differential diagnosis of an adrenal mass that does not show lipid includes metastasis, pheochromocytoma, adrenocortical carcinoma, and rare tumors such as ganglioneuroma.

Adrenal masses that show signal intensity loss on opposed-phase images are most commonly adrenal adenomas. Myelolipomas usually demonstrate focal fat (identified with fat saturation sequences) but may also show focal or diffuse admixtures of myeloid and fat cells, which result in an appearance identical to that of adenomas. However, the clinical significance of incidental myelolipomas is similar to that of adenomas. Uncommonly, myelolipomas may hemorrhage, which complicates the radiologic appearance (Fig 11).

Figure 11. Hemorrhagic myelolipoma of the right adrenal gland in a 76-year-old woman. **(a, b)** In-phase (120/4.2) **(a)** and opposed-phase (120/2.7) **(b)** MR images show a large, heterogeneous mass with areas that are hyperintense relative to the spleen. One area (arrow) shows decreased signal intensity on the opposed-phase image **(b)**, a finding consistent with lipid. Note that the hyperintense areas in the hematoma (*H*) due to blood do not demonstrate signal intensity loss on the opposed-phase image **(b)**. **(c)** Axial T2-weighted fast spin-echo MR image (10,000/104) shows that the mass is hypointense, an appearance that proved to represent hematoma (*H*) at surgery. However, the nodule that was hypointense on the opposed-phase image **(b)** has become hyperintense (arrow). **(d)** Sagittal T1-weighted fat saturation MR image (150/2.2) shows the mass displacing the kidney with no evident enhancement. *H* = hematoma. **(e)** Photomicrograph (original magnification, ×40; hematoxylin-eosin stain) of the mass shows clear adipose cells and myeloid tissue (arrowheads) interspersed with adrenocortical cells.

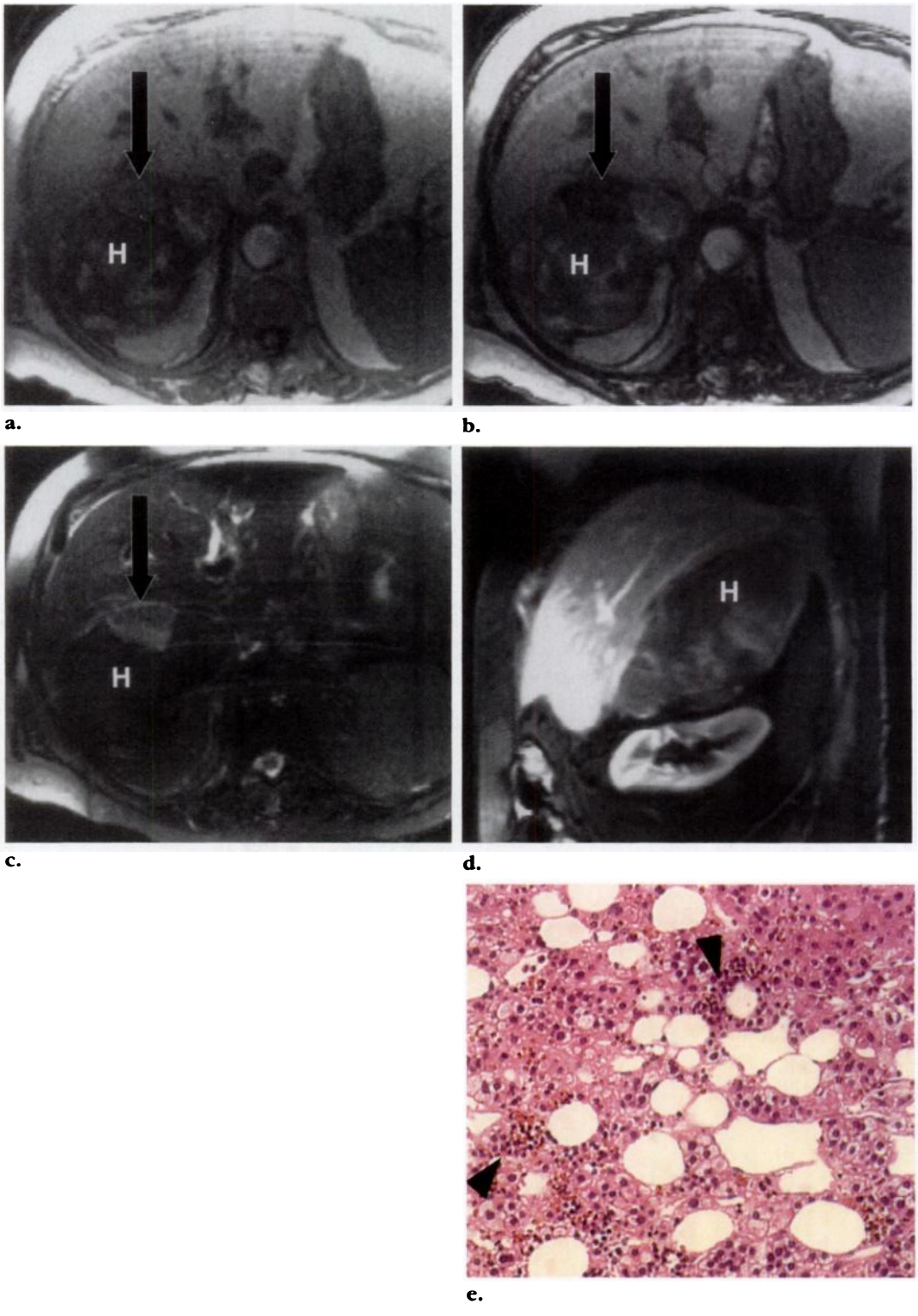

Figure 12. Angiomyolipoma of the right kidney in a 45-year-old woman. **(a)** In-phase T1-weighted MR image (120/4.2) shows a hyperintense renal mass (*aml*). This degree of high signal intensity in a mass is consistent with fat or hemorrhage. **(b)** Opposed-phase T1-weighted MR image (120/2.1) shows that some areas of the mass remain hyperintense (arrow) and some demonstrate signal intensity loss (*aml*). **(c)** Fat saturation opposed-phase T1-weighted MR image (120/2.1) shows markedly decreased signal intensity compared with that on the in-phase image **(a)**, a finding that indicates predominantly fatty tissue. **(d)** Water saturation T1-weighted MR image (120/4.2) shows markedly decreased signal intensity in the area of hemorrhage. *aml* = angiomyolipoma.

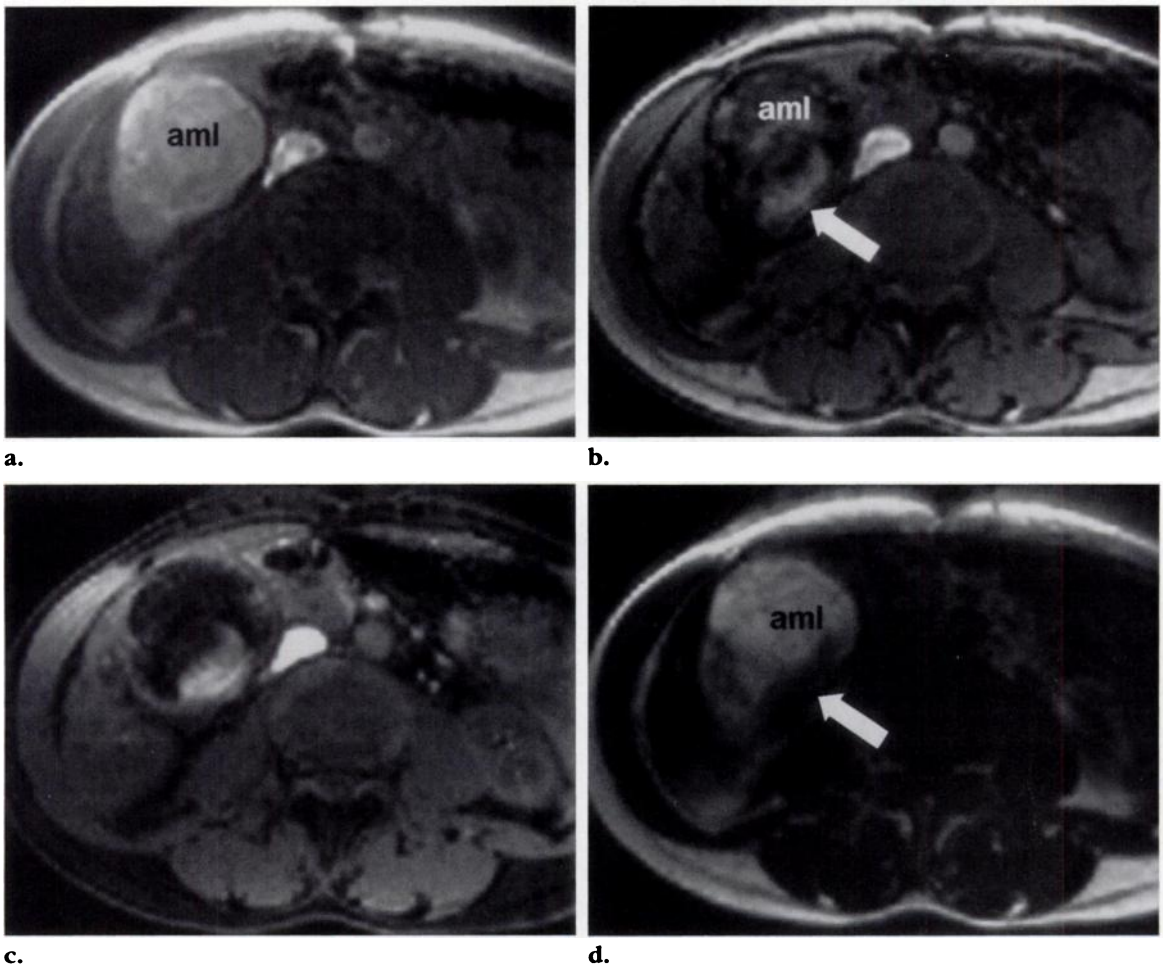

a. **b.**

c. **d.**

At histologic analysis, adrenocortical carcinoma can appear similar to adrenal adenoma. Lipid-rich cells may be present, although they are usually admixed with other histologic types. A case of adrenocortical carcinoma has been reported in which there was an area of signal intensity loss on opposed-phase images (25), although it is clear that the majority of adrenocortical carcinomas do not show this finding (26). In any case, the vast majority of adrenocortical carcinomas are large and necrotic and would not be confused with adrenal adenomas.

• Renal Tumors

Angiomyolipomas frequently occur in the kidneys and contain variable amounts of vascular, muscle, and fatty tissue. These tumors usually demonstrate focal fat at CT or MR imaging, a finding that makes the diagnosis straightforward. Angiomyolipomas should be evaluated with conventional fat-suppressed imaging instead of opposed-phase imaging because the former technique is more sensitive in detection of predominantly fatty foci and the latter is more sensitive in detection of small proportions of lipid within a voxel (Fig 12). Uncommonly, angiomyolipomas do not contain fat (27,28).

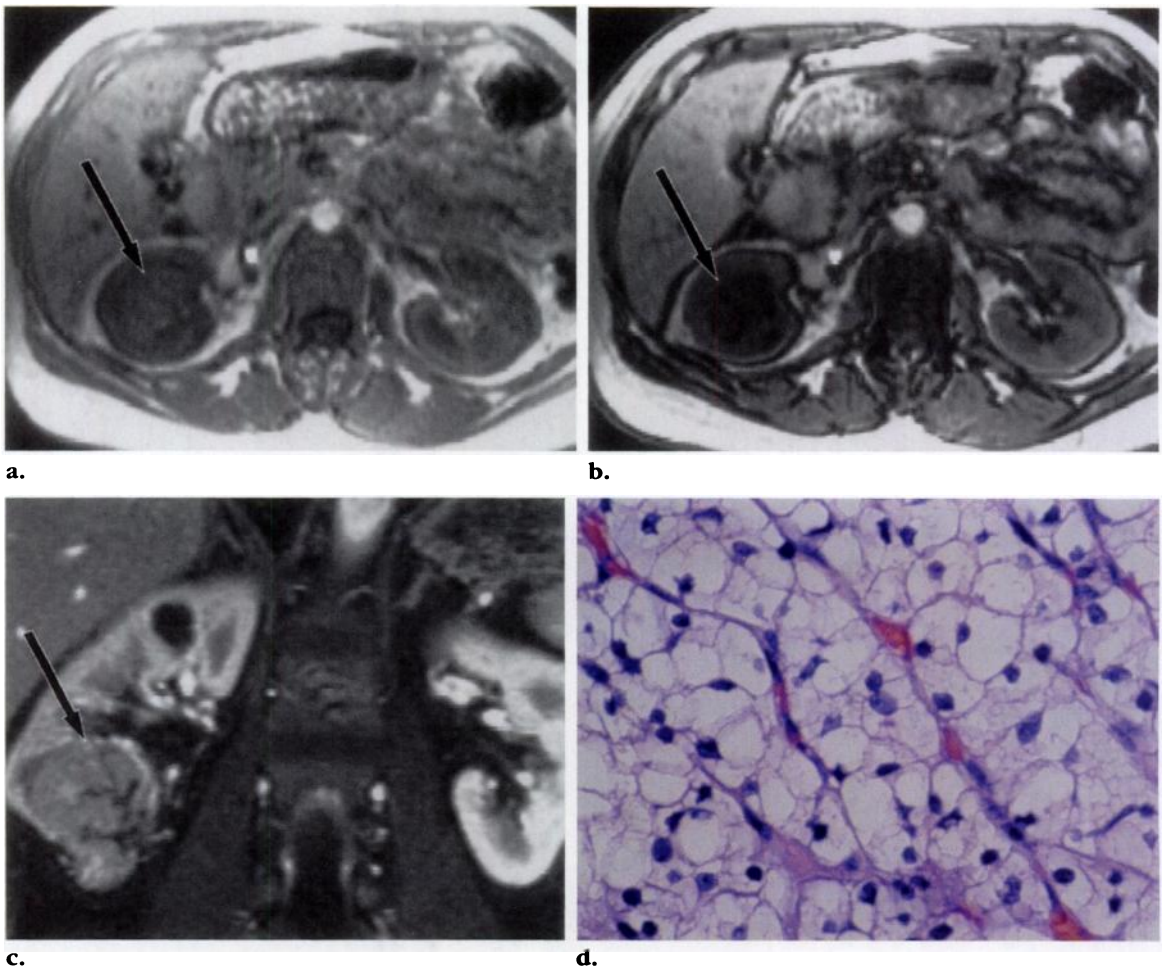

Figure 13. Clear cell renal carcinoma in a 50-year-old woman. **(a)** In-phase MR image (120/4.2) shows a mass in the lower pole of the right kidney (arrow). The mass is slightly hyperintense relative to the adjacent kidney tissue. **(b)** Opposed-phase MR image (120/2.1) shows that the mass (arrow) is hypointense relative to the adjacent kidney tissue, a finding that indicates lipid. **(c)** Coronal gadolinium-enhanced fat saturation gradient-echo MR image (70/1.6) shows diffuse enhancement throughout the lesion (arrow); this finding indicates that the mass represents perfused tissue. **(d)** Photomicrograph (original magnification, ×400; hematoxylin-eosin stain) of the tumor shows clear cells.

However, the presence of fat is not diagnostic proof of angiomyolipoma. A minority of clear cell renal carcinomas show diminished signal intensity on opposed-phase images relative to that on in-phase images (29) (Fig 13). This finding presumably results from the intracellular lipid known to be present in these tumors. Renal cell carcinomas of other cell types such as granular cell, as well as other renal tumors such as oncocytoma, transitional cell carcinoma, and lymphoma, do not contain such lipid (Fig 14). More rarely, calcified renal cell carcinomas may show tiny foci of fat (27,30,31). However, the presence of focal fat, as opposed to the patchy or diffuse lipid seen on opposed-phase images, in a noncalcified mass can still be considered diagnostic of angiomyolipoma.

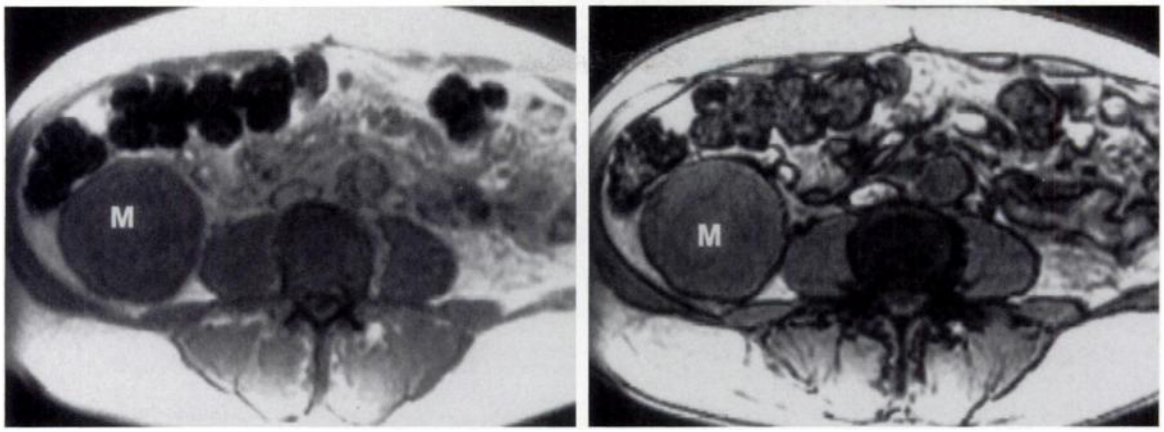

a. b.

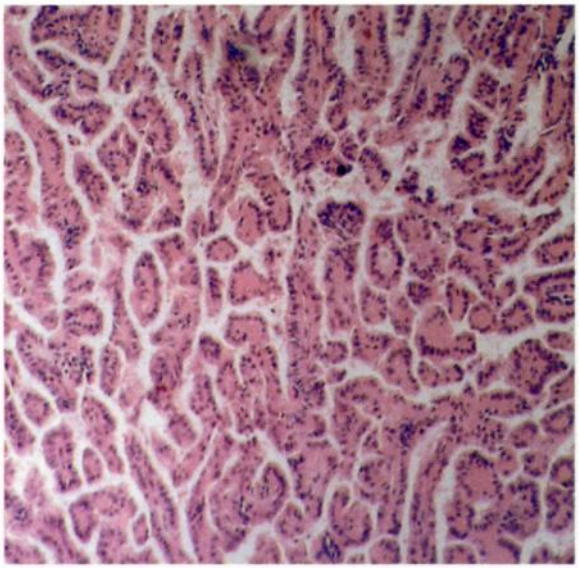

c.

Figure 14. Papillary granular cell carcinoma of the kidney in a 73-year-old man. **(a, b)** In-phase (120/4.2) **(a)** and opposed-phase (100/2.3) **(b)** MR images show a large mass (*M*) in the lower pole of the right kidney. The signal intensity of the mass in **b** is unchanged relative to the signal intensity in **a**. Thus, there is no evidence of lipid in this lesion. **(c)** Photomicrograph (original magnification, ×40; hematoxylin-eosin stain) of the tumor shows papillary granular cells but no clear cells.

■ SUMMARY

Opposed-phase gradient-echo MR images are sensitive to relatively small amounts of lipid in tissues and can be used to identify lipid-containing tumors such as hepatocellular tumors, adrenal adenomas, and clear cell renal carcinomas. Both in-phase and opposed-phase images should be acquired with similar parameters because unequivocal identification of lipid in tissues requires comparison with in-phase images to control for T1 and T2* effects and because opposed-phase imaging may obscure lesions. In liver masses, the presence of lipid is largely restricted to primary hepatocellular tumors. Renal and adrenal masses may contain focal fat (angiomyolipomas and myelolipomas, respectively) or diffuse lipid (clear cell renal carcinomas and adenomas, respectively). Therefore, it is important to distinguish the lipid identified on opposed-phase images from focal fat, which is better demonstrated on fat-saturated T1-weighted images.

■ REFERENCES

1. Dixon WT. Simple proton spectroscopic imaging. Radiology 1984; 153:189–194.
2. Leroy-Willig A, Duboc D, Bittoun J, et al. Spectroscopic MRI: a tool for the evaluation of systemic lipid storage disease. Magn Reson Imaging 1990; 8:511–515.
3. Levenson H, Greensite F, Hoefs J, et al. Fatty infiltration of the liver: quantification with phase-contrast MR imaging at 1.5 T vs biopsy. AJR 1991; 156:307–312.
4. Chan TW, Listerud J, Kressel HY. Combined chemical-shift and phase-selective imaging for fat suppression: theory and initial clinical experience. Radiology 1991; 181:41–47.
5. Szumowski J, Eisen JK, Vinitski S, Haake PW, Plewes DB. Hybrid methods of chemical-shift imaging. Magn Reson Med 1989; 9:379–388.
6. Wehrli FW, Perkins TG, Shimakawa A, Roberts F. Chemical shift-induced amplitude modulations in images obtained with gradient refocusing. Magn Reson Imaging 1987; 5:157–158.

7. Tsushima Y, Dean PB. Characterization of adrenal masses with chemical shift MR imaging: how to select echo times (letter). Radiology 1995; 195:285-286.
8. Fishbein MH, Gardner KG, Potter CJ, Schmalbrock P, Smith MA. Introduction of fast MR imaging in the assessment of hepatic steatosis. Magn Reson Imaging 1997; 15:287-293.
9. Mitchell DG, Stolpen AH, Siegelman ES, Bolinger L, Outwater EK. Fatty tissue on opposed-phase MR images: paradoxical suppression of signal intensity by paramagnetic contrast agents. Radiology 1996; 198:351-357.
10. Mitchell DG, Kim I, Chang TS, et al. Fatty liver: chemical shift phase-difference and suppression magnetic resonance imaging techniques in animals, phantoms, and humans. Invest Radiol 1991; 26:1041-1052.
11. Kreft BP, Tanimoto A, Baba Y, et al. Diagnosis of fatty liver with MR imaging. JMRI 1992; 2: 463-471.
12. Martin J, Sentis M, Puig J, et al. Comparison of in-phase and opposed-phase GRE and conventional SE MR pulse sequences in T1-weighted imaging of liver lesions. J Comput Assist Tomogr 1996; 20:890-897.
13. Mitchell DG, Palazzo J, Hann HW, Rifkin MD, Burk DL Jr, Rubin R. Hepatocellular tumors with high signal on T1-weighted MR images: chemical shift MR imaging and histologic correlation. J Comput Assist Tomogr 1991; 15: 762-769.
14. Mathieu D, Paret M, Mahfouz AE, et al. Hyperintense benign liver lesions on spin-echo T1-weighted MR images: pathologic correlations. Abdom Imaging 1997; 22:410-417.
15. Paulson EK, McClellan JS, Washington K, Spritzer CE, Meyers WC, Baker ME. Hepatic adenoma: MR characteristics and correlation with pathologic findings. AJR 1994; 163:113-116.
16. Chung KY, Mayo-Smith WW, Saini S, Rahmouni A, Golli M, Mathieu D. Hepatocellular adenoma: MR imaging features with pathologic correlation. AJR 1995; 165:303-308.
17. Martin J, Sentis M, Zidan A, et al. Fatty metamorphosis of hepatocellular carcinoma: detection with chemical shift gradient-echo MR imaging. Radiology 1995; 195:125-130.
18. Martin J, Falco J, Donoso L, Puig J, Zidan A, Sentis M. Hepatic angiomyolipoma: value of proton (fat/water) chemical shift fast low angle shot (FLASH) MR imaging technique in detecting fatty tissue content. Magn Reson Imaging 1995; 13:903-906.
19. Outwater EK, Siegelman ES, Radecki PD, Piccoli CW, Mitchell DG. Distinction between benign and malignant adrenal masses: value of T1-weighted chemical-shift MR imaging. AJR 1995; 165:579-583.
20. Mitchell DG, Crovello M, Matteucci T, Petersen RO, Miettinen MM. Benign adrenocortical masses: diagnosis with chemical shift MR imaging. Radiology 1992; 185:345-351.
21. Schwartz LH, Panicek DM, Koutcher JA, et al. Adrenal masses in patients with malignancy: prospective comparison of echo-planar, fast spin-echo, and chemical shift MR imaging. Radiology 1995; 197:421-425.
22. Bilbey JH, McLoughlin RF, Kurkjian PS, et al. MR imaging of adrenal masses: value of chemical-shift imaging for distinguishing adenomas from other tumors. AJR 1995; 164:637-642.
23. Korobkin M, Lombardi TJ, Aisen AM, et al. Characterization of adrenal masses with chemical shift and gadolinium-enhanced MR imaging. Radiology 1995; 197:411-418.
24. Mayo-Smith WW, Lee MJ, McNicholas MM, Hahn PF, Boland GW, Saini S. Characterization of adrenal masses (< 5 cm) by use of chemical shift MR imaging: observer performance versus quantitative measures. AJR 1995; 165:91-95.
25. Schlund JF, Kenney PJ, Brown ED, Ascher SM, Brown JJ, Semelka RC. Adrenocortical carcinoma: MR imaging appearance with current techniques. JMRI 1995; 5:171-174.
26. Leroy-Willig A, Bittoun J, Luton JP, et al. In vivo MR spectroscopic imaging of the adrenal glands: distinction between adenomas and carcinomas larger than 15 mm based on lipid content. AJR 1989; 153:771-773.
27. Hélénon O, Merran S, Paraf F, et al. Unusual fat-containing tumors of the kidney: a diagnostic dilemma. RadioGraphics 1997; 17:129-144.
28. Uhlenbrock D, Fischer C, Beyer HK. Angiomyolipoma of the kidney: comparison between magnetic resonance imaging, computed tomography, and ultrasonography for diagnosis. Acta Radiol 1988; 29:523-526.
29. Outwater EK, Bhatia M, Siegelman ES, Burke MA, Mitchell DG. Lipid in renal clear cell carcinoma: detection on opposed-phase gradient-echo MR images. Radiology 1997; 205:103-107.
30. Strotzer M, Lehner KB, Becker K. Detection of fat in a renal cell carcinoma mimicking angiomyolipoma. Radiology 1993; 188:427-428.
31. Radin DR, Chandrasoma P. CT demonstration of fat density in renal cell carcinoma. Acta Radiol 1992; 33:365-367.